Flow-Level Simulation for Adaptive Routing Protocols in Vehicular Ad-Hoc Networks

Kais Elmurtadi Suleiman(✉) and Otman Basir

Electrical and Computer Engineering, University of Waterloo, Waterloo, ON, Canada
{kelmurta,obasir}@uwaterloo.ca

Abstract. Adaptive routing reacts to a varying connected vehicle density by switching between different routing techniques (e.g. from Instant routing under high densities to delay-tolerant routing under low densities). These adaptations take place over large scales of time and space which makes their simulation challenging computationally. Flow-level simulators can address such challenges by using the right level of abstraction. In this paper, we present a flexible and extendable flow-level simulation environment for adaptive routing protocols in Vehicular Ad-hoc NETworks (VANETs). We discuss in details the different networking and mobility modules involved using rigorous mathematical modeling. We use MATLAB as the language of choice which allows researchers to utilize our environment while harnessing MATLAB's statistics and machine learning libraries. Such sophisticated libraries are a critical toolbox for adaptive routing protocol researchers. To the best of our knowledge, no such simulator has been publicly accessible so far.

Keywords: Flow-level · Simulation · Adaptation · Routing · VANET

1 Introduction

1.1 Adaptive Routing

Throughout different spaces and times of deployment, VANETs can be at one of three network states with a varying connected vehicles density as shown in Fig. 1. In State-1, vehicles can only communicate through the infrastructure. In State-2, vehicles can communicate through the infrastructure and other scattered vehicles. In State-3, vehicles can use both V2I and V2V communication efficiently given the small voids between vehicles. Depending on the state, different routing techniques would be suitable ranging from Multi-tier routing using V2I communication to Delay-tolerant routing, Instant routing and others using V2V communication. Adaptive routing enables switching between these different routing techniques in response to variations in the connected vehicles density.

Commonly used adaptive routing techniques include: Multi-tier routing, Instant routing, Delay-tolerant routing, Cluster-based routing, Cross-layer Optimized routing, Terminated routing, Expedited routing, Splitted routing and

Y. Zhou and T. Kunz (Eds.): AdHocNets 2017, LNICST 223, pp. 94–105, 2018.
https://doi.org/10.1007/978-3-319-74439-1_9

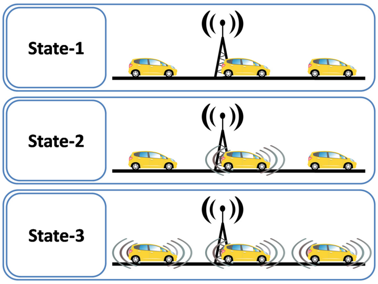

Fig. 1. VANET states

Redundant routing. **Multi-tier routing** takes place between different network tiers with different radio access technologies. **Delay-tolerant routing** overcomes big voids by storing, carrying and forwarding packets. **Instant routing** routes data instantly via optimal paths given a high connected-vehicle density. **Cluster-based routing** groups vehicle members around vehicle cluster heads. **Cross-layer optimized routing** takes into consideration information coming from other network layers. **Terminated routing** terminates packet forwarding after their Time-To-Live (TTL) period expires or after a certain number of hops is passed. **Expedited routing** forwards popular content packets before they are requested. **Splitted routing** splits packets between different paths and **Redundant routing** sends redundant packet copies using the same path or different paths.

Different adaptive routing protocols implement different sets of routing techniques and different adaptation mechanisms. A famous example is the Spray and Wait routing protocol proposed in [1]. This protocol adapts between Instant, Redundant and Delay-tolerant routing techniques. This is done by sending L message copies to L neighbors in the Spraying phase while simply transmitting messages directly to the destination in the Waiting phase if the destination has not yet been reached. Another well-known example is the Mobility-centric Data Dissemination algorithm for Vehicular networks (MDDV) proposed in [2]. This protocol adapts between Instant, Delay-tolerant and Terminated routing techniques by allowing vehicles to decide: what to send, when to send and whether to store or drop messages.

1.2 Flow-Level Simulation

As we can see, adaptive routing protocols allow for successful VANET deployment throughout different network states by switching between different routing techniques. However, this wide operational span in terms of both space and time makes their simulation challenging computationally. Flow-level simulators can address such challenges by using the right level of abstraction. Contrary to packet-level simulators, flow-level simulators deal with the data traffic as a flow inside the network. This approach makes them an efficient tool that gives a quick estimation of the network status while acknowledging the fact that it is impractical to simulate all details. Figure 2 depicts the flow-level simulation model for buffers where the current status depends on both the incoming and outgoing rates. We shall discuss this more rigorously using mathematical modeling next in the paper.

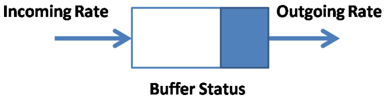

Fig. 2. Flow-level buffer model

1.3 Paper Organization

In Sect. 2, we go through some related work in order to highlight the contributions made afterwards in Sect. 3. Our simulation environment is explained in details in Sect. 4 including the simulation scenario and modules. Finally, we present in Sect. 5 some sample results in order to validate this environment.

2 Related Work

Few flow-level simulators have been proposed for high speed networks. In [3], Venkataramanan et al. propose a flow-model simulator for the internet while Yan and Gong in [4] propose a time-driven flow-level simulator for high speed networks in which traffic is treated as fluids inside the network. To the best of our knowledge, no flow-level simulator has ever been proposed for VANETs in general and for adaptive routing protocols in specific. Boban and Vinhoza in [5] focus on modeling vehicle signal obstacles while Kaisser et al. in [6] propose an enhancement for the well-known packet-level simulator "OPNET" that allows integration with the mobility simulator "SUMO". Liu et al. in [7] propose "VGSim"; an integrated mobility and networking simulation environment for VANETs also based on packet-level simulation. They claim that their simulator is the first of its kind in terms of integrating both networking and mobility aspects of VANET simulation. In both [8,9], enhancements are proposed for packet-level VANET simulators; in [8], an extension for SUMO's TafficModeller program has been presented which allows for easy traffic simulation on the network simulator "Veins" using "OpenStreetMaps". In [9], Naoumov and Gross propose an enhancement for the packet-level simulator "NS2" based on exploiting signal propagation properties. Conventional simulation platforms such as NS, OMNET++ or OPNET provide packet-level simulations which, despite the high accuracy, may struggle with a large number of nodes. Moreover, these platforms do not provide an integrated mobility and networking platform for VANET simulation. They are also not as rich as MATLAB in terms of providing efficient statistics and machine learning toolboxes which we claim to have a high potential for adaptive routing protocol research.

3 Contributions

Given the above discussion and as it is shown in the next sections, we believe that our contributions can be summarized as follows:

- Presenting an efficient and scalable flow-level simulation environment for adaptive routing protocols in VANETs. This environment is flexible and extendable in terms of adopting new scenarios and modules. It allows for fair and valid comparisons between different VANET adaptive routing protocols,
- Providing a rigorous mathematical modeling for the simulation modules,
- Covering both mobility and networking aspects of simulation which makes our simulation environment self-reliant, and
- Using MATLAB as the language of choice which allows researchers to use our environment while utilizing MATLAB's sophisticated statistics and machine learning libraries. We believe that such libraries are of high importance for adaptive routing protocol research.

4 Simulation Environment

Although other scenarios and simulator modules can easily be implemented, we restrict ourselves in this paper, due to space constraints, to the highway simulation scenario shown in Fig. 3 and the overall simulator structure shown in Fig. 4.

4.1 Scenario

Our simulation runs for a duration S_T in steps of $\triangle t$. A total of NV vehicles in the set $\mathbf{V}$ are distributed uniformly between N_L highway lanes. Each lane starts at X_{min}, ends at X_{max} and has a width of L_W. Each vehicle $V_i \in \mathbf{V}$ travels continuously while generating a constant bit rate CBR traffic with a broadcasting range of V_{BR}. The Road Side Units (RSUs) are IRD apart and located midway. The cellular access point is also located midway at (AP_X, AP_Y). Given advances in today's location services, we assume that each vehicle knows about the positions of: the access point, the RSUs and all neighboring vehicles.

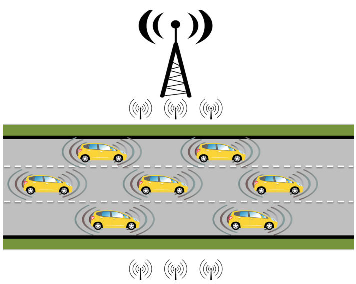

Fig. 3. Simulation scenario

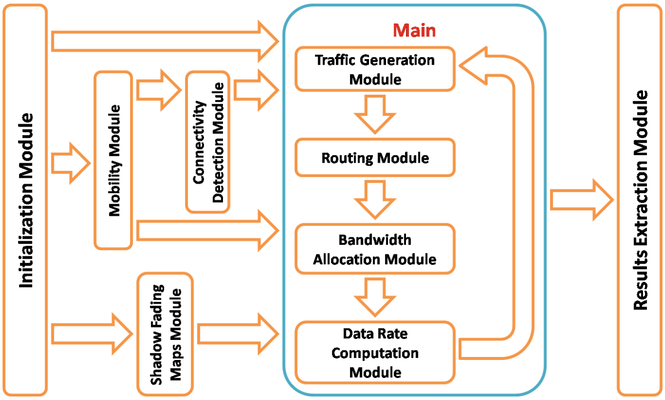

Fig. 4. Simulator structure

4.2 Simulator Structure

Initialization Module. Initial parameter assumptions are made here including those related to the overall simulation scenario and other simulator modules as summarized in Table 1.

Mobility Module. This modules generates vehicle mobility traces given the initial assumptions of the corresponding parameters mentioned in Table 1. Initially, $\{V_{X_1}, ..., V_{X_{NV}}\}$ are set uniformly randomly between X_{min} and X_{max} and $\{V_{Y_1}, ..., V_{Y_{NV}}\}$ fall in the middle of a lane chosen at random. Speeds $\{V_{S_1}, ..., V_{S_{NV}}\}$ are set uniformly randomly between V_{Smin} and V_{Smax} and accelerations $\{V_{A_1}, ..., V_{A_{NV}}\}$ are set uniformly randomly between 0 and $MaxVA$. Driver behavior parameters $\{V_{B_1}, ..., V_{B_{NV}}\}$ are set uniformly randomly between 0 and 1/2. After each $\triangle t$, V_{S_i} for all vehicles is updated as follows:

- $V_{S_i}(t + \triangle t) = min(V_{S_i}(t) + V_{A_i}, V_{Smax})$ if:
  - V_i is at least Dis_{max} length units behind the same-lane front vehicle, or
  - V_i is at least Dis_{max} length units behind a neighboring-lane front vehicle. In which case, V_i changes to this lane before accelerating.
- $V_{S_i}(t + \triangle t) = max(V_{S_i}(t) - V_{A_i}, V_{Smin})$ if:
  - V_i is at most Dis_{min} length units behind the same-lane front vehicle and less than Dis_{max} length units behind both neighboring-lane front vehicles.
- Otherwise:

$$V_{S_i}(t + \triangle t) = \begin{cases} V_{S_i}(t), & w/prob: 1 - 2 \times V_{B_i} \\ min(V_{S_i}(t) + V_{A_i}, V_{Smax}), & w/prob: V_{B_i} \\ max(V_{S_i}(t) - V_{A_i}, V_{Smin}), & w/prob: V_{B_i} \end{cases}$$

Table 1. Simulation parameters

	Item	Symbol		Item	Symbol
Scenario parameters					
	Simulation time	S_T		Lane width	L_W
	Time step	$\triangle t$		Vehicle broadcasting range	V_{BR}
	Number of lanes	N_L		Inter-RSU distance	IRD
	Minimum X-position	X_{min}		Access point X-position	AP_X
	Maximum X-position	X_{max}		Access point Y-position	AP_Y
Mobility Module parameters					
	Minimum vehicle speed	V_{Smin}		Minimum inter-vehicle distance	Dis_{min}
	Maximum vehicle speed	V_{Smax}		Maximum inter-vehicle distance	Dis_{max}
	Maximum vehicle acceleration	$MaxVA$			
Shadow Fading Maps Module parameters					
Cellular	decorrelation distance	C_{Dcorr}	Vehicular	decorrelation distance	V_{Dcorr}
Cellular	shadow fading mean	SF_{CM}	Vehicular	shadow fading mean	SF_{VM}
Cellular	shadow fading standard deviation	SF_{CSD}	Vehicular	shadow fading standard deviation	SF_{VSD}
Data Rate Computation Module parameters					
Access point	carrier frequency	AP_{Freq}	Vehicle	carrier frequency	$V2V_{Freq}$
Access point	bandwidth	AP_{BW}	Vehicle	bandwidth	$V2V_{BW}$
Access point	Physical resource block bandwidth	PRB_{BW}	Vehicle	transmission power level	V_P
			Vehicle	antenna-azimuth pattern	$V_{A(\theta)}$
Access point	transmission power level	AP_P	Vehicle	antenna gain	V_{AG}
Access point	antenna-azimuth pattern	$AP_{A(\theta)}$	Vehicle	antenna height	V_{AH}
Access point	antenna gain + cable loss	AP_{AG}	Vehicle	cable loss	V_{CLoss}
			Vehicle	cable length	V_{CL}
	Noise figure	NF		Thermal noise density	TND

After updating V_{S_i}, V_{X_i} is updated as follows:
$V_{X_i}(t+\triangle t) = V_{X_i}(t) + \triangle t \times V_{S_i}(t+\triangle t)$
where: $V_{X_i}(t+\triangle t) \leftarrow V_{X_i}(t+\triangle t) - X_{max}\, if\, V_{X_i}(t+\triangle t) > X_{max}$

Connectivity Detection Module. Given the generated mobility traces, this module produces traces of all vehicle reachable neighbors including other vehicles and RSUs. These reachable neighbors set traces are needed by the Routing Module and the Bandwidth Allocation Module. Given $V_i \in \mathbf{V}$ located at (V_{X_i}, V_{Y_i}), this module constructs V_i neighbors set $\mathbf{V}_{N_i}$ by first excluding V_i and any neighboring V_j located at (V_{X_j}, V_{Y_j}) if V_j is located more than V_{BR} length units away from V_i as follows:

$$\mathbf{V}_{N_i} = \mathbf{V} \cup \mathbf{R} - \{V_i\} - \{V_j \in \mathbf{V} | ((V_{X_i} - V_{X_j})^2 + (V_{Y_i} - V_{Y_j})^2)^{\frac{1}{2}} > V_{BR}\}$$

where $\mathbf{R}$ is the set of all RSUs. After these exclusions, this module excludes neighboring V_j from $\mathbf{V}_{N_i}$ if there is another V_k obstructing the line of sight communication between V_j and V_i as follows:

$$\mathbf{V}_{N_i} \leftarrow \mathbf{V}_{N_i} - \{V_k \in \mathbf{V} | \\ (((V_{X_i} - V_{X_k})^2 + (V_{Y_i} - V_{Y_k})^2)^{\frac{1}{2}} < ((V_{X_i} - V_{X_j})^2 + (V_{Y_i} - V_{Y_j})^2)^{\frac{1}{2}}) \\ \wedge (|(V_{X_i} - V_{X_k})|/|(V_{Y_i} - V_{Y_k})| = |(V_{X_i} - V_{X_j})|/|(V_{Y_i} - V_{Y_j})|) \\ \wedge sgn(V_{X_i} - V_{X_k}) = sgn(V_{X_i} - V_{X_j}) \wedge sgn(V_{Y_i} - V_{Y_k}) = sgn(V_{Y_i} - V_{Y_j})\}$$

The same type of exclusions applies between V_i and any $R_w \in \mathbf{R}$.

Shadow Fading Maps Module. Using the same method adopted by [10], this module computes the correlated shadow fading map values SF_C given the initial parameter assumptions mentioned in Table 1. It starts by computing the uncorrelated values SF_U for both cellular and vehicular networks as follows:

$$10 \times log_{10}(SF_U) = SF_M + SF_{SD} \times randn$$

where SF_M and SF_{SD} are the corresponding shadow fading mean and standard deviation in dBs, respectively and "$randn$" represents a normally-distributed random number. The map sizes are given by: $[\frac{X_{max}-X_{min}}{C_{Dcorr}}] \times [\frac{AP_Y}{C_{Dcorr}}]$ for the cellular network and $[\frac{X_{max}-X_{min}}{V_{Dcorr}}] \times [\frac{AP_Y}{V_{Dcorr}}]$ for the vehicular network.

Given the distances $Xpos$ and $Ypos$ and the four SF_U values shown in Fig. 5, this module computes SF_C at (X, Y) as follows:

$$SF_C(X,Y) = (1 - \frac{Xpos}{Dcorr})^{\frac{1}{2}}(SF_{U,0}(\frac{Ypos}{Dcorr})^{\frac{1}{2}} + SF_{U,3}(1 - \frac{Ypos}{Dcorr})^{\frac{1}{2}}) \\ + (\frac{Xpos}{Dcorr})^{\frac{1}{2}}(SF_{U,1}(\frac{Ypos}{Dcorr})^{\frac{1}{2}} + SF_{U,2}(1 - \frac{Ypos}{Dcorr})^{\frac{1}{2}})$$

this applies for both cellular and vehicular networks where $Dcorr$ represents the corresponding decorrelation distance (i.e. C_{Dcorr} or V_{Dcorr}).

Traffic Generation Module. Given the vehicle buffers $V_{Buff_{i,i}}(t = 0) = 0\, \forall V_i \in \mathbf{V}$, this module generates the incoming flow rate represented by CBR for each vehicle V_i as follows, where $V_{Buff_{i,i}}$ is the V_i data stored at V_i buffer: $V_{Buff_{i,i}}(t + \triangle t) = V_{Buff_{i,i}}(t) + CBR \times \triangle t$.

Routing Module. Given $V_{Buff_{i,i}}$ and $\mathbf{V}_{N_i}$ of each vehicle, this module forwards data according to the implemented routing protocol.

Bandwidth Allocation Module. Given the routing decisions made, this module divides bandwidth between the contending vehicles. This is shown throughout the next Data Rate Computation Module.

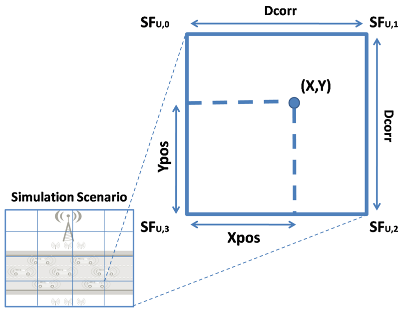

Fig. 5. Shadow fading map computation (reproduced from [4])

Data Rate Computation Module. Given the bandwidth allocations, all vehicles and access point locations, SF_C values of both cellular and vehicular networks and the initial assumptions of the corresponding parameters mentioned in Table 1, this module computes data rates and then updates vehicle buffers accordingly. For the cellular network, we adopt the OFDM access scheme, the LTE path loss model proposed by [11] and Shannon's capacity formula. For the vehicular network, we adopt the same assumptions except for using the path loss model proposed by [12] instead. Starting with the cellular network, this module allocates the bandwidth V_{BW_i} to each V_i and computes the thermal noise V_{N_i} as follows:

$$V_{BW_i} = \lfloor AP_{BW}/(NV \times PRB_{BW}) \rfloor \times PRB_{BW}$$
$$10 \times log_{10}(V_{N_i}) = TND + 10 \times log_{10}(V_{BW_i}) + NF$$

The distance $Dis_{i,AP}$ between V_i and the access point is computed followed by computing the signal path loss V_{PL_i} as follows:

$$Dis_{i,AP} = ((V_{X_i} - AP_X)^2 + (V_{Y_i} - AP_Y)^2)^{\frac{1}{2}}$$
$$V_{PL_i} = 128.1 + 37.6 \times log_{10}(Dis_{i,AP}) - 37.6 \times log_{10}(1000) + SF_C(AP_X, AP_Y)$$

The signal strength V_{S_i} is computed afterwards in order to compute the cellular network data rate V_{CDR_i} representing the outgoing flow rate and then update vehicle buffer statuses as follows:

$$10 \times log_{10}(V_{S_i}) = V_P + V_{AG} + V_{A(\theta)} + AP_{AG} - V_{CL} \times V_{CLoss} + AP_{A(\theta)} - V_{PL_i}$$
$$V_{CDR_i} = V_{BW_i} \times log_2(1 + V_{S_i}/V_{N_i})$$
$$V_{Buff_{i,i}}(t + \triangle t) = max(V_{Buff_{i,i}}(t) - V_{CDR_i}, 0)$$

For the vehicular network, the thermal noise for each V_i and the distance $Dis_{i,j}$ between V_i and V_j are computed as follows:

$$10 \times log_{10}(V_{N_i}) = TND + 10 \times log_{10}(V2V_{BW}/|\mathbf{V}_{PP_i}|) + NF$$
$$Dis_{i,j} = ((V_{X_i} - V_{X_j})^2 + (V_{Y_i} - V_{Y_j})^2)^{\frac{1}{2}}$$

where $\mathbf{V}_{PP_i}$ is the set of vehicle data paths passing through V_i. Before computing the signal path loss $V_{PL_{i,j}}$ between V_i and V_j, the breaking point distance BPD is computed using the parameters $V2V_{Freq}, V_{AH}$ and V_λ as follows:

$$V_\lambda = (3 \times 10^8)/V2V_{Freq}$$
$$BPD = (4 \times V_{AH}^2 - V_\lambda^2/4)/V_\lambda$$
$$V_{PL_{i,j}} = \begin{cases} 58.7 + 1.66 \times 10 \times log_{10}(Dis_{i,j}) + SF_C(V_{X_j}, V_{Y_j}), \\ if\ Dis_{i,j} < BPD \\ 58.7 + 1.66 \times 10 \times log_{10}(BPD/10) + SF_C(V_{X_j}, V_{Y_j}) \\ +2.88 \times 10 \times log_{10}(Dis_{i,j}/BPD), \\ if\ Dis_{i,j} \geq BPD \end{cases}$$

Using $V_{PL_{i,j}}$ and knowing $\mathbf{V}_{PP_i}$, the signal strength $V_{S_{i,j}}$ at V_j received from V_i is computed using the formula:

$$10 \times log_{10}(V_{S_{i,j}}) =$$
$$V_P - 10 \times log_{10}(|\mathbf{V}_{PP_i}|) - V_{PL_{i,j}} + 2 \times (V_{AG} + V_{A(\theta)} - V_{CL} \times V_{CLoss})$$

The outgoing flow rate represented by the vehicular network data rate V_{VDR_i} is computed afterwards and before updating V_i data at both V_i and V_j buffer statuses as follows:

$$V_{VDR_i} = V2V_{BW}/|\mathbf{V}_{PP_i}| \times log_2(1 + V_{S_{i,j}}/V_{N_i})$$
$$V_{Buff_{j,i}}(t + \triangle t) = V_{Buff_{j,i}}(t) + min(V_{VDR_i}, V_{Buff_{i,i}}(t))$$
$$V_{Buff_{i,i}}(t + \triangle t) = max(V_{Buff_{i,i}}(t) - V_{VDR_i}, 0)$$

With an intermediate vehicle V_k in the data path, we have:

$$V_{VDR_i} = min(V_{VDR_i}(E_{V_i,V_k}) + V_{VDR_i}(E_{V_k,V_j}))$$
$$V_{Buff_{j,i}}(t + \triangle t) = V_{Buff_{j,i}}(t) + min(V_{VDR_i}, V_{Buff_{k,i}}(t))$$
$$V_{Buff_{k,i}}(t + \triangle t) = max(V_{Buff_{k,i}}(t) - V_{VDR_i}, 0)$$

where E_{V_i,V_k} is the data path edge between V_i and V_k.

Results Extraction Module. This module extracts final results in the form of traces and plots. These traces and plots can be accustomed to collect specific information throughout simulation.

5 Sample Results

As a proof-of-concept and in order to validate our flow-level simulation environment, we simulate a representative adaptive routing protocol and compare its performance to that of its individual routing techniques, namely: Multi-tier,

Algorithm 1. Representative adaptive routing protocol

while V_i is ON **do**
  Route $V_{Buff_{i,i}}$ using *Multi-tier routing*;
  if $(V_{Buff_{i,i}} > V_{CDR_i})$ **then**
    if $(\mathbf{V}_{Path_i} \neq \emptyset)$ **then**
      Route $(V_{Buff_{i,i}} - V_{CDR_i})$ using *Instant routing*;
    else
      if $Time \leq Monitoring\,Period$ **then**
        Compute $P(\mathbf{V}_{Path_i} \neq \emptyset)$;
        Route $(V_{Buff_{i,i}} - V_{CDR_i})$ using *Delay-tolerant routing*;
      else
        if $P(\mathbf{V}_{Path_i} \neq \emptyset) < \alpha$ **then**
          Route $(V_{Buff_{i,i}} - V_{CDR_i})$ using *Delay-tolerant routing*;
        end if
      end if
    end if
  end if
  Route $(V_{Buff_{i,j}} > 0 \forall V_j)$ using *Delay-tolerant routing*;
end while

Instant and Delay-tolerant routing. Algorithm 1 shows the pseudocode of this protocol while leaving the technical details of its individual routing techniques for future work due to space constraints.

Using our adaptive routing protocol, each vehicle forwards its data using Multi-tier routing. If there is still data remaining $(V_{Buff_{i.i}} > V_{CDR_i})$, then the protocol routes this data using Instant routing if there is an instant path $(\mathbf{V}_{Path_i} \neq \emptyset)$ or using Delay-tolerant routing if there isn't and the probability of finding one is less than a threshold $(\alpha = \frac{1}{3})$ once the "*Monitoring Period*" has passed. The "*Monitoring Period*" is the period during which $P(\mathbf{V}_{Path_i} \neq \emptyset)$ is monitored/computed while relying on Delay-tolerant routing if: $(V_{Buff_{i.i}} > V_{CDR_i}) \wedge (\mathbf{V}_{Path_i} = \emptyset)$. This condition is implemented in order to avoid a more congested delay-tolerant path while waiting for a less congested instant path estimated to come shortly with $(P(\mathbf{V}_{Path_i} \neq \emptyset) \geq \alpha)$. In all cases, any $(V_{Buffi,j} > 0)$ is always routed using Delay-tolerant routing. Results in Fig. 6a to c validate our simulation environment by meeting our intuitions as follows:

- Multi-tier routing provides a declining data rate due to the increasing congestion occurring at the access point,
- Instant routing provides a growing data rate due to the higher probability of finding instant paths as the number of vehicles increases. The slight contention level increase is due to the growing path competition,
- Delay-tolerant routing starts with a fast growing data rate that quickly struggles under the pressure of more vehicles. This is due to the fact that the delay-tolerance exhibited allows for communications under low vehicle density while incurring the cost of a quickly rising contention level that jeopardizes eventually the data rate,

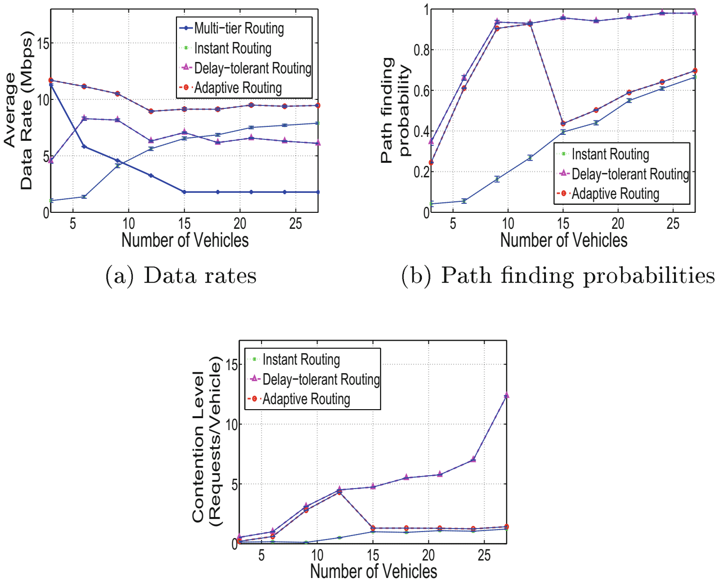

(a) Data rates

(b) Path finding probabilities

(c) Contention levels

Fig. 6. Adaptive routing performance against its individual routing techniques

– Our adaptive routing protocol utilizes initially Multi-tier routing. Then, it finds delay-tolerant paths by switching to Delay-tolerant routing. However, it switches afterwards to Instant routing as the contention level rises after exceeding 12 vehicles. After 12 vehicles, the probability of finding an instant path surpasses the threshold ($\alpha = \frac{1}{3}$) which we set as acceptable given the benefit of avoiding high contention levels under Delay-tolerant routing.

6 Conclusions and Future Work

Adaptive routing protocols allow for successful VANET deployment by switching between different routing techniques. However, their operational span makes their simulation computationally demanding. Flow-level simulators offer the right level of abstraction in order to overcome such computational challenges.

In this paper, we have presented a flow-level simulation environment for adaptive routing in VANETs with its different modules explained using rigorous mathematical modeling. These modules include both VANET networking and mobility aspects which makes our environment self-reliant. MATLAB has been chosen in order to allow researchers in the field to utilize our environment while harnessing the rich MATLAB statistics and machine learning libraries needed for adaptive routing research. In order to validate our environment, we have evaluated the performance of a representative adaptive routing protocol against its individual routing techniques. Results confirm our intuitions and show the adaptations made. In the future, we plan to extend our environment in order to simulate and develop adaptive routing techniques which utilize MATLAB's statistics and machine learning libraries. Finally, plans are underway to make our environment publicly accessible online.

References

1. Spyropoulos, T., Psounis, K., Raghavendra, C.S.: Spray and wait: an efficient routing scheme for intermittently connected mobile networks. In: Proceedings of the 2005 ACM SIGCOMM Workshop on Delay-Tolerant Networking (WDTN 2005), pp. 252–259. ACM, New York (2005)
2. Wu, H., Fujimoto, R., Guensler, R., Hunter, M.: MDDV: a mobility-centric data dissemination algorithm for vehicular networks. In: Proceedings of the 1st ACM International Workshop on Vehicular Ad hoc Networks (VANET 2004), pp. 47–56. ACM, New York (2004)
3. Venkataramanan, R., Jeong, M.-W., Prabhakar, B.: A Flow-and Packet-level Model of the Internet
4. Yan, A., Gong, W.-B.: Time-driven fluid simulation for high-speed networks. IEEE Trans. Inf. Theory **45**(5), 1588–1599 (1999)
5. Boban, M., Vinhoza, T.T.V.: Modeling and simulation of vehicular networks: Towards realistic and efficient models. INTECH Open Access Publisher (2011)
6. Kaisser, F., Gransart, C., Berbineau, M.: Simulations of VANET scenarios with OPNET and SUMO. In: Vinel, A., Mehmood, R., Berbineau, M., Garcia, C.R., Huang, C.-M., Chilamkurti, N. (eds.) Nets4Cars/Nets4Trains 2012. LNCS, vol. 7266, pp. 103–112. Springer, Heidelberg (2012). https://doi.org/10.1007/978-3-642-29667-3_9
7. Liu, B., Khorashadi, B., Du, H., Ghosal, D., Chuah, C., Zhang, M.: VGSim: An integrated networking and microscopic vehicular mobility simulation platform. IEEE Commun. Mag. **47**(5), 134–141 (2009)
8. Arellano, W., Mahgoub, I.: TrafficModeler extensions: A case for rapid VANET simulation using, OMNET++, SUMO, and VEINS. In: High Capacity Optical Networks and Emerging/Enabling Technologies. Magosa 2013, pp. 09–115 (2013)
9. Naoumov, V., Gross, T.: Simulation of large ad hoc networks. In: Proceedings of the 6th ACM International Workshop on Modeling Analysis and Simulation of Wireless and Mobile Systems (MSWIM 2003), pp. 50–57. ACM, New York (2003)
10. IEEE 802.16: EEE 802.16m Evaluation Methodology Document (EMD). IEEE 802.16 Broadband Wireless Access Working Group, January 2009
11. Astely, D., Dahlman, E., Furuskar, A., Jading, Y., Lindstrom, M., Parkvall, S.: LTE: the evolution of mobile broadband. IEEE Commun. Mag. **47**(4), 44–51 (2009)
12. Abbas, T., Kåredal, J., Tufvesson, F.: Shadow fading model for vehicle-to-vehicle network simulators. In: COST IC1004 5th Management Committee and Scientific Meeting, COST IC1004 (2012)